

Ionization of low-Rydberg-state He atoms by polar molecules. I. Velocity dependence of the cross sections

C. Ronge, A. Pesnelle, M. Perdrix, and G. Watel

*Service de Physique des Atomes et des Surfaces, Centre d'Etudes Nucléaires de Saclay,
91191 Gif-sur-Yvette Cédex, France*

(Received 22 December 1987; revised manuscript received 4 April 1988)

The ionization of low-Rydberg-state He atoms in the n^1P state ($n=14$) in collisions with the polar molecules NH_3 , SO_2 , and acetone ($\text{C}_3\text{H}_6\text{O}$) is carried out in a crossed-beam experiment at thermal kinetic energies. The dependence of the experimental ionization cross sections σ_i^{exp} on the relative velocity of the reactants is obtained by a time-of-flight method. We observe that it varies mainly as $1/v^2$ in a large part of the studied velocity range, while a $1/v$ velocity dependence is predicted by the free-electron model for the higher Rydberg levels.

I. INTRODUCTION

Quenching processes taking place in collisions between a Rydberg atom $A^*(nl)$ and a polar-molecule (M) target have been largely studied in several laboratories,¹ mainly for highly excited levels $n > 30$. Momentum transfer (state changing) such as l mixing and n changing

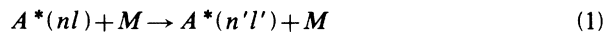
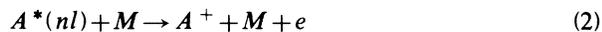


exhibit large cross sections; collisional ionization (CI)



takes place also in such collisions but has been much less studied than momentum transfer.

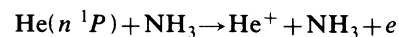
One of the aims of these studies was to test the validity of the model based on reducing the interactions solely to that between the Rydberg electron and the molecule and therefore disregarding the interaction between the core A^+ and the molecule; the electron is assumed to behave as if it were free with a kinetic energy equal to that relevant to its orbital motion. It is the so-called "free-electron model," largely developed by Matsuzawa² for this kind of collision involving Rydberg atoms; in this model, the electron-molecule interaction is usually treated in the dipole-Born approximation. Flannery,³ Latimer,⁴ Petitjean and Gounand⁵ have also based their approach on the same hypothesis; convenient analytical formulas have been calculated by Petitjean and Gounand⁵ enabling a rapid comparison of this model with experimental results.

Several experimental measurements on polar molecules, such as NH_3 and HF , have been carried out by Kellert *et al.*⁶ and Higgs *et al.*⁷ with $\text{Xe}^*(nl)$ ($22 < n < 40$) as a projectile; recently, Kalamarides *et al.* extended their measurements⁸ to $\text{Rb}(ns)$ for $40 < n < 48$. In both cases, they measure rate constants as a function of n for state-changing collisions, and mainly conclude that their data substantiate the free-electron model. However, it is worth noting that, while the data on state-changing rate constants were well reproduced with such

calculations, data⁶ presented on collisional ionization by NH_3 exceeded the calculation values by about a factor of 3.

Total collisional depopulation through l -mixing, n -changing, and collisional-ionization processes of $\text{Rb}^*(ns)$ and $\text{Rb}^*(nd)$ ($24 \leq n \leq 49$) by NH_3 has been studied by Petitjean *et al.*⁹ They measured quenching cross sections as a function of n and compared them with theoretical calculations using the free-electron model. It can be observed that the variations versus n of the cross sections calculated for $\text{Rb}(nd)$ levels exhibit a maximum around $n \approx 47$ due to l mixing induced by NH_3 inversion, as observed in the experimental data. For $\text{Rb}(ns)$ levels, the agreement is not so good: the calculations indicate a strong increase around $n \approx 36$ which is not as well reproduced by the experimental data as in the case of nd levels. A quantitative comparison between theory and experiment shows that the analytical formulas generally overestimate the cross sections by one-half to one order of magnitude: this can be understood when considering the simplicity of the model, and the agreement can be still viewed as reasonable. However, in the experiment on $\text{Xe}(nf) + \text{NH}_3$ made by Kellert *et al.*,⁶ the calculated cross-section increase due to l mixing induced by NH_3 inversion is not observed.

We had observed¹⁰ a very high ionization He^+ signal in collisions of He^* with ammonia



for the low Rydberg states $14 \leq n \leq 16$. Such an ionization signal could not be predicted at all in the framework of the free-electron model proposed by Matsuzawa. Especially, the use of the dipole-Born approximation to treat the electron-polar-molecule interaction induces a selection rule for the transitions of rotational deexcitation of the molecule: $\Delta J = -1$, $\Delta K = 0$. The binding energy of the Rydberg electron reaches 558.8 cm^{-1} for $n=14$. Such an energy can be delivered only in transitions from rotational levels $J \geq 30$ and these levels are not populated in our thermal NH_3 distribution at 300 K.

We are consequently inclined to think that (i) even if the free-electron model gives a satisfying order of magnitude for total depopulation rate constants and cross sections versus n , it is perhaps not suitable for a more precise description of the interactions during these collisions; (ii) the ability of this model to describe the interactions correctly certainly decreases as n decreases, due to the approximations involved (in particular, the impulse approximation); the study of low Rydberg states is then instructive; (iii) the Rydberg-atom-molecule interactions should be viewed in a frame larger than that used in the free-electron model; and (iv) a more refined experimental investigation of the process, such as the dependence of the cross sections with the relative velocity of the reactants, will provide additional information which could better explain the Rydberg-molecule collisions.

We present here the result of such a measurement on the systems $\text{He}(14^1P) + M \rightarrow \text{He}^+ + M + e$, with $M = \text{NH}_3$, SO_2 , and $\text{C}_3\text{H}_6\text{O}$ (acetone). These molecules have been chosen for their interesting set of dipole and rotational constant values. NH_3 and SO_2 have nearly the same dipole but very different rotational constants; SO_2 and $\text{C}_3\text{H}_6\text{O}$ have rotational constants of the same order of magnitude but dipole values in the ratio $\frac{1}{2}$. This measurement is made in a crossed-beam apparatus using a time-of-flight technique, in order to obtain the velocity dependence of the collisional-ionization cross section.

II. EXPERIMENT

A. Experimental setup

The ionization of $\text{He}(14^1P)$ at thermal kinetic energies is carried out in a three-crossed-beam apparatus, using a time-of-flight (TOF) technique (see Fig. 1). A 3-mm-diam

collimated $\text{He}(2^1S, 2^3S)$ metastable beam issuing from a discharge source, a laser beam for excitation from the 2^1S metastable level to the 14^1P level, and a 4-mm-diam collimated molecular beam issuing from a multicapillary array intersect perpendicularly in a mass-spectrometer chamber.

We have used the TOF technique many times in this apparatus, either for Penning ionization^{11,12} or Hornbeck-Molnar ionization^{12,13} cross-section measurements; using a sophisticated version of this technique, simultaneous measurements of the TOF spectra of the He^+ ions produced during the collision and of the fluorescence photons emitted by the $\text{He}(14^1P)$ atoms decaying to the ground state 1^1S , used to monitor the excited-state population, are performed; they yield the variations of the cross section as a function of the relative velocity v , (then of the relative kinetic energy E_{kin}) of the reactants. Several improvements were introduced for the purpose of the present measurements, details of which are given here.

1. Laser excitation of $\text{He}(14^1P)$

Excitation of the $\text{He}(14^1P)$ level from the $\text{He}(2^1S)$ metastable level requires a narrow-bandwidth uv radiation at 317.7 nm. This is generated by intracavity frequency doubling [i.e., second-harmonic generation (SHG)] in a single-mode ring dye laser as for previous experiments.¹⁴ However, this time the dye and the crystal are different and the SHG performances have been considerably enhanced. The laser is operated with sulforhodamine-B (Kiton Red), a dye which is usually used in pulsed lasers; this dye, in a cw single-mode laser, proves to be much more efficient and stable than dicyanomethylene-2-methyl-6(*p*-dimethylaminostyryl)-4-

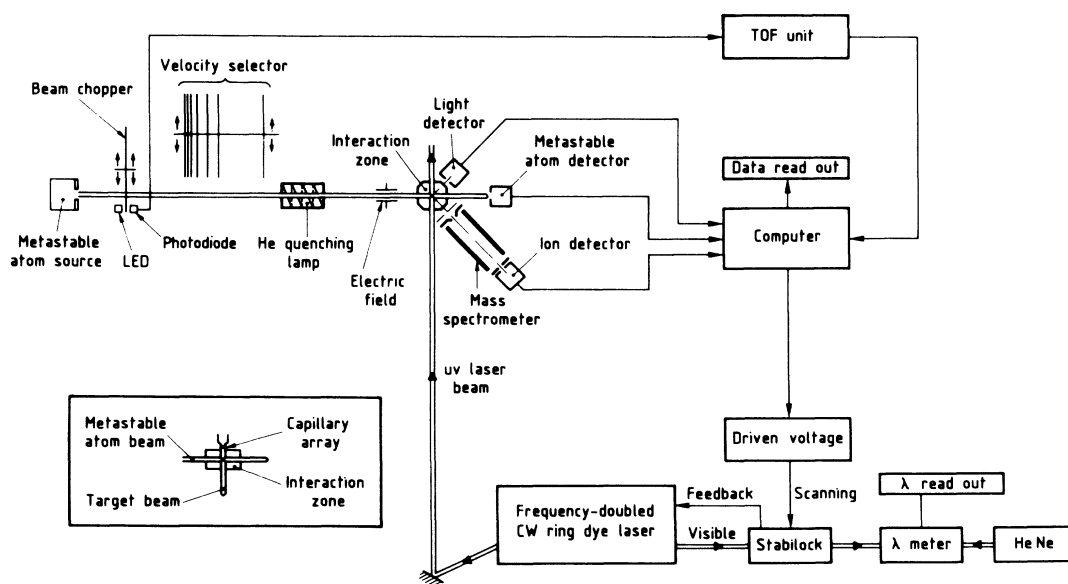


FIG. 1. Schematic representation of the time-of-flight, crossed-beam apparatus in a horizontal plane; in the inset, in a vertical plane.

H-pyran (DCM), which was the recommended dye for required wavelength range. Using a 4-cm-long rubidium dihydrogen phosphate (RDP) crystal, in noncritical 90° phase matching, we obtain up to 45 mW of 317.7-nm uv radiation, single mode and stabilized over several hours, with an all-lines Ar⁺ pump laser power equal to 11 W.

In order to excite the whole He* velocity range, we adjust the angular divergence of the uv beam to that of the He* metastable beam, $\alpha = 1.8 \times 10^{-4}$ rad, by means of a 500-mm-focal-length lens. The uv light spot size in the interaction region is 1.5 mm [full width at half maximum (FWHM)] and then smaller than the diameters of both the He* metastable and the target beams. The averaged excitation efficiency $2^1S \rightarrow 14^1P$ is estimated to be of the order of 20%.

2. Interaction region

The three metastable, laser, and target beams intersect perpendicularly in the mass-spectrometer chamber. Their intersection defines the interaction region. The optical excitation region is located inside the metastable target atom beam intersection, since the He(14^1P) lifetime is as short as 0.163 29 μ s (Ref. 15) and the excited He atoms travel through a mean distance of only 0.3 mm in the target gas, where they undergo ionizing collisions, before decaying principally to the 1^1S level; these atoms are therefore finally lost for the process. This strong 50.6-nm fluorescence light is detected on a channeltron multiplier, equipped with a 15-mm-diam cone in order to obtain a large detection solid angle. This fluorescence detection is used to monitor the laser excited He atom population which is different from the metastable one, since all the velocities present in the metastable beam are not excited to the same extent.¹² This is due to the fact that the excited-state population depends on the time of exposure of the He metastable atoms to the laser light, which means that the faster the metastable atom, the lower will be the excitation efficiency.

The metastable atoms are detected downstream on an electron multiplier. When a perfect tuning of the uv laser is achieved, the fluorescence signal is at its maximum; the He(2^1S) metastable signal is consequently at its minimum, due to the very short lifetime of the He(14^1P) excited atom which prevents it from reaching the detector.

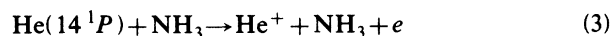
Simultaneously with the fluorescence detection, the ions are detected after being extracted from the interaction chamber and mass selected by a quadrupole mass spectrometer; this detection is effected on a channeltron multiplier after the ions' trajectory is turned at 90° at the quadrupole exit in order to avoid the background signal due to the fluorescence photons.

B. Experimental procedure

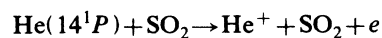
1. Ion and fluorescence photon measurements

In order to obtain the collisional-ionization cross section as a function of the relative velocity v_r of the reactants, we detect as a function of time of flight τ , for a given pressure of target gas, the following.

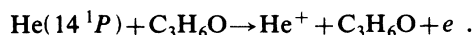
(i) The He⁺ ions produced in the following reactions:



or



or



(ii) The fluorescence photons emitted by the He(14^1P) atoms decaying to the ground state 1^1S .

Because of possible spatial and temporal laser power fluctuations, both signals are detected simultaneously in order to guarantee good reproducibility and reliability of our results. We checked the following points in order to define a satisfactory experimental procedure.

(i) The transition probability for spontaneous decay from He(14^1P) to the ground state is extremely high as compared with other decay possibilities:¹⁶ $A_{14P-1S} = 5.802 \times 10^6 \text{ s}^{-1}$. Figure 2 shows that the proportion of 14^1P decaying to 1^1S , equal to $A_{14P-1S} \times T_{14P}$, is 95%. The 50.6-nm fluorescence signal consequently monitors the excited atom population efficiently.

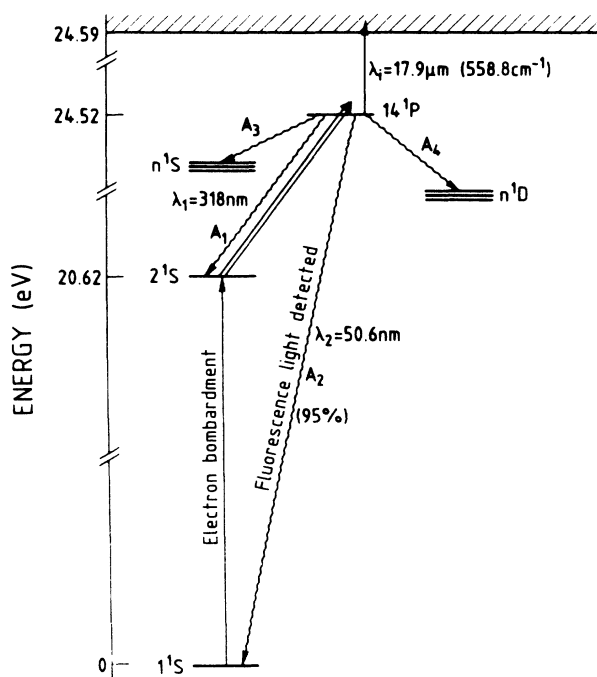


FIG. 2. Partial term diagram showing the relevant levels for the experiment and scheme of the two-step excitation and deexcitation of the He(14^1P) level. The A_i ($1 \leq i \leq 4$), noted on the figure, are equal to the A_{ij} or the sum of the A_{ij} Einstein coefficients for deexcitation on the 1^1S , 2^1S , n^1D ($3 \leq n \leq 13$), and n^1S ($3 \leq n \leq 13$) levels: $A_1 = 1.845 \times 10^5 \text{ s}^{-1}$, $A_2 = 5.802 \times 10^6 \text{ s}^{-1}$, $A_3 = 1.037 \times 10^5 \text{ s}^{-1}$, and $A_4 = 3.486 \times 10^4 \text{ s}^{-1}$ (Ref. 16).

(ii) We observe a background signal (laser off) on the fluorescence detector, of the order of 10% of the fluorescence signal, due to the scattering of the metastable atoms by the target molecules. This signal is taken into account in the derivation of the ionization cross section $\sigma_{\text{eff}}^{\text{expt}}(v)$.

(iii) We observe a background signal on the ion detector (laser on, target pressure $P=0$ Torr) due to He^+ ions produced from $\text{He}(14^1P)$ by two ionization processes: by collisions on the residual background gas in the interaction chamber, and by interaction with 300-K blackbody radiation. This signal is also considered in the derivation of $\sigma_{\text{eff}}^{\text{expt}}(v)$.

The experimental procedure adopted is thus as follows:

(i) for a given target pressure P , we simultaneously record on the TOF analyzer both fluorescence $N^*(\tau)$ and He^+ ion $N^+(\tau)$ TOF spectra, with the laser tuned on the transition (laser on); (ii) for the same target pressure, we record the background fluorescence $I_{\text{BG}}^*(\tau)$ with the laser off; and (iii) for $P=0$ Torr, we simultaneously record both $N^*(\tau)$ and $N^+(\tau)$ spectra (laser on); for $P=0$ Torr, $I_{\text{BG}}^*(\tau)$ is negligible (laser off). The contribution of the TOF signals to the cross section is therefore [see formula (8)]

$$\sigma_{\text{eff}}^{\text{expt}}(\tau) \sim \tau \left[\frac{N^+(\tau)}{N^*(\tau) - I_{\text{BG}}^*(\tau)} \right]_P - \left[\frac{N^+(\tau)}{N^*(\tau)} \right]_{P=0}. \quad (4)$$

2. Importance of the choice of target gas pressure

Since multicollision processes, for instance, the ionizing collision being preceded by n -changing transitions, could be responsible for ionization, it is important to investigate carefully the dependence of the He^+ signal on the target gas density. This density cannot be measured inside the interaction chamber; the gauge is located upstream from the multicapillary array and indicates a pressure P . In the interaction zone, the pressure is thus several orders of magnitude smaller than P .

In a first step, we verified that the target gas density ρ in the interaction zone was proportional to the pressure P (for $P \leq 0.2$ Torr) by measuring the M^+ ions produced by Penning ionization of the target gas in collisions with metastable He atoms (laser off), $\text{He}(2^1S, 2^3S) + M \rightarrow M^+ + \text{He} + e$, as a function of the pressure P . We did in fact observe a linear dependence of the M^+ signal on the pressure P for the three NH_3 , SO_2 , and $\text{C}_3\text{H}_6\text{O}$ target molecules, which guarantees that $P \sim \rho$. In a second step, for a given velocity $v=2400$ m/s of the helium atoms, which is the most probable velocity in our beam, we investigated the dependence of the He^+ ion signal on upstream gas pressure P . This was done by setting up a movable mechanical velocity selector on the He^* beam, which is not used for the TOF measurements, having a resolution of about 10%. A linear dependence, indicative of a one-collision ionizing mechanism, is observed in the following ranges: $0 \leq P \leq 0.04$ Torr for NH_3 (see Fig. 3)

and for $\text{C}_3\text{H}_6\text{O}$, $0 \leq P \leq 0.05$ Torr for SO_2 . We selected the following values for P (measured upstream from the multicapillary array) to make our TOF measurements: $P=0.03$ Torr for NH_3 and $\text{C}_3\text{H}_6\text{O}$, $P=0.04$ Torr for SO_2 , these being pressures for which the collisional-ionization signal is maximum in the linear part.

C. Time-of-flight formulas

Each of the channels of a TOF spectrum of nominal time of flight τ corresponds to a velocity v of the He atom such that $v=L/\tau$, L being the flight path between the chopper and the interaction zone. All the formulas can then be written directly as a function of v instead of τ . Let $\phi^*(v)$ (expressed in $\text{cm}^{-2} \text{s}^{-1}$) and $n^*(v)$ (expressed in cm^{-3}) be, respectively, the flux and the density of the excited He atoms in the interaction zone. They are related directly by

$$n^* = \phi^* / v. \quad (5)$$

1. Fluorescence signal

In the interaction zone, the uv $2^1S \rightarrow 14^1P$ photoexcitation of the helium atoms creates a number of excited

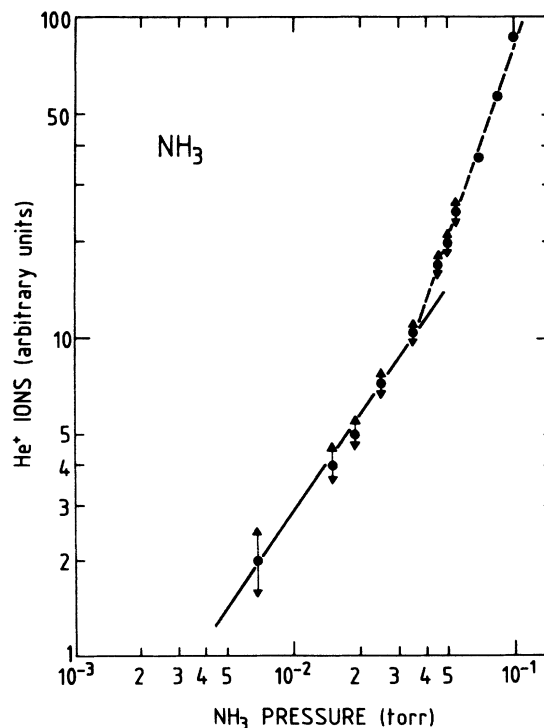


FIG. 3. NH_3 pressure dependence of the He^+ ion signal for ionizing $\text{He}(14^1P) + \text{NH}_3$ collisions [reaction (3)] relevant to the same fluorescence signal intensity; closed circles, measurements; solid line, calculated linear variation (slope 1 in log-log coordinates); dashed line, calculated quadratic variation (slope 2 in log-log coordinates). The P value is that measured upstream from the multicapillary array.

atoms emitting fluorescence photons with the decay rate A_{14P-1S} which, at 95%, is equal to $1/T_{14P}$ (see Sec. II B 1). The TOF fluorescence signal [number of counts in the channel τ of width $\delta(\tau)$, corresponding to the velocity v] is given by

$$N^*(v) = \frac{R\Omega}{4\pi T_{14P}} \delta\tau \int \int \int_{V_1} n^*(v; x, y, z) dx dy dz ,$$

where $\delta\tau$ is the channel width, Ω is the solid angle of fluorescence light detection, R the 50.6-nm photon detection efficiency, and V_1 the three-beam intersection volume. Taking into account formula (5), we obtain

$$N^*(v) = \frac{R\Omega}{4\pi T_{14P}} \delta\tau \frac{1}{v} \int \int \int_{V_1} \phi^*(v; x, y, z) dx dy dz . \quad (6)$$

2. He⁺ ion signal and effective ionization cross section $\sigma_{\text{eff}}^{\text{expt}}(v)$

The ions produced in the collision defined by (3) are detected by an electron multiplier after being mass selected; the relevant TOF signal is given by

$$N^+(v) = k\rho\sigma_{\text{eff}}^{\text{expt}}(v)\delta\tau \int \int \int_{V_1} \phi^*(v; x, y, z) dx dy dz , \quad (7)$$

where k is the collection efficiency of our experimental system, including collecting coefficient and mass analyzer transmission, ρ is the total density of target molecules in the interaction region, and $\sigma_{\text{eff}}^{\text{expt}}(v)$ is the so-called experimental effective ionization cross section.

Comparing the N^* and N^+ signals, we derive

$$\sigma_{\text{eff}}^{\text{expt}}(v) = \frac{\Omega R}{4\pi k\rho T_{14P}} \left[\frac{N^+(v)}{vN^*(v)} \right] .$$

In fact, when we take into account the background signals (see Sec. II B 1), the cross section is derived by

$$\sigma_{\text{eff}}^{\text{expt}}(v) = \frac{\Omega R}{4\pi k\rho T_{14P}v} \left[\left[\frac{N^+(v)}{N^*(v) - I_{\text{BG}}^*(v)} \right]_{\rho} - \left[\frac{N^+(v)}{N^*(v)} \right]_{\rho=0} \right] . \quad (8)$$

3. Experimental ionization cross section $\sigma_i^{\text{expt}}(v_r)$

The experimental effective ionization cross section $\sigma_{\text{eff}}^{\text{expt}}(v)$ is expressed as a function of the He velocity v . It is related to the experimental ionization cross section $\sigma_i^{\text{expt}}(v_r)$, as a function of the relative velocity of the reactants v_r , by

$$\sigma_i^{\text{expt}}(v_r) = v\sigma_{\text{eff}}^{\text{expt}}(v)/v_r . \quad (9)$$

In this formula, v_r is defined via the He velocity v , the target velocity v_t , and the velocity distribution of the target molecules; it has been shown¹¹ that (9) provides $\sigma_i^{\text{expt}}(v_r)$ within a good accuracy. For each value of v , v_r

is calculated and $\sigma_i^{\text{expt}}(v_r)$ is derived by formula (9). Let us mention here that the difference between $\sigma_i^{\text{expt}}(v_r)$ and $\sigma_{\text{eff}}^{\text{expt}}(v)$ is negligible for SO₂ and C₃H₆O, which are much heavier than He; for NH₃ there is a small difference located only in the low velocity range 1000–2500 m/s.

III. EXPERIMENTAL RESULTS

The TOF spectra for an upstream NH₃ pressure $P=0.03$ Torr (which guarantees a one-collision ionization process; see Sec. II B 2) are reported in Fig. 4 as a function of the time of flight τ . The cross section $\sigma_i^{\text{expt}}(v_r)$ is plotted on Fig. 5 as a function of the relative velocity v_r . We observe that $\sigma_i^{\text{expt}}(v_r)$ does not vary as $1/v_r$, as predicted in the free-electron model. A variation of $\sigma_i^{\text{expt}}(v_r)$ as approximately $1/v_r^2$ is observed in a large part (1100 $\leq v_r \leq 3000$ m/s) of the studied velocity range; for $v_r \geq 3000$ m/s, the variation with v_r is still stronger.

The same curves are obtained for SO₂ (upstream SO₂ pressure $P=0.04$ Torr) and for C₃H₆O (upstream pressure $P=0.03$ Torr). The cross sections are shown in Figs. 6 and 7. The same comments as for NH₃ can be made

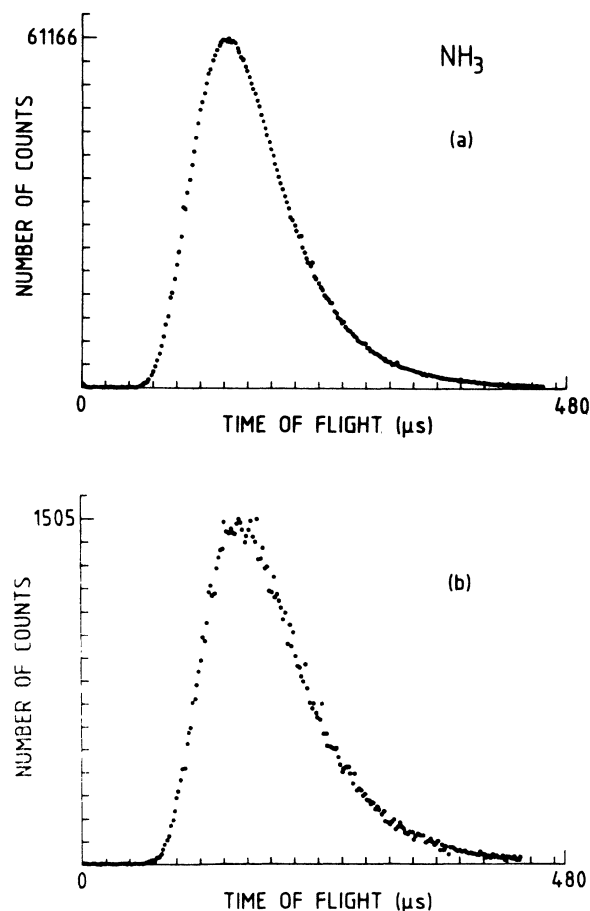


FIG. 4. TOF spectra used to extract the ionization cross section for He(¹⁴P) + NH₃ collisions (channel width is 2 μs). (a) Fluorescence photons; (b) He⁺ ions produced in the collision [reaction (3)].

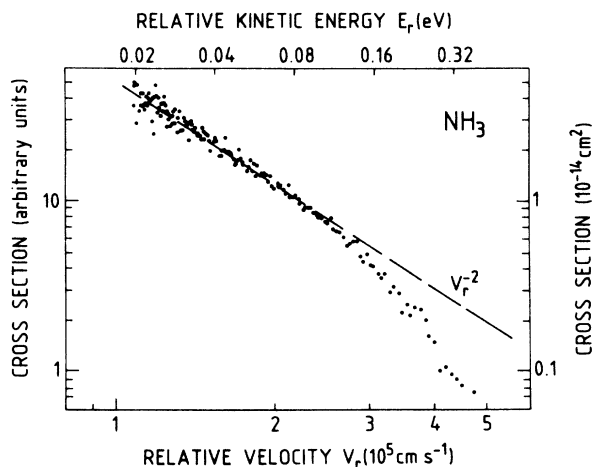


FIG. 5. Experimental ionization cross section $\sigma_i^{\text{exp}}(v_r)$ for $\text{He}(14^1P) + \text{NH}_3$ collisions [reaction (3)] as a function of the relative velocity and kinetic energy of the reactants. Dashed line, calculated function $1/v_r^2$. The absolute scale shown on the right-hand side of the figure is obtained experimentally by a method described in the following paper (Ref. 21).

since the curves giving the velocity dependence of both cross sections for NH_3 and SO_2 are superimposed (without considering any absolute value); however, in the case of $\text{C}_3\text{H}_6\text{O}$, the shape is slightly different from that due to NH_3 and SO_2 . As a comment, the three studied molecules are not exactly equivalent since, in addition to their different dipole values, NH_3 is a pure symmetric-top molecule and SO_2 a very slightly asymmetric-top molecule (near the limiting case of a prolate symmetric top), while $\text{C}_3\text{H}_6\text{O}$ is a true asymmetric-top molecule.¹⁷

IV. DISCUSSION AND CONCLUSION

The fact that the velocity dependence of the ionization cross section does not follow the behavior expected from the free-electron model calls for several comments.

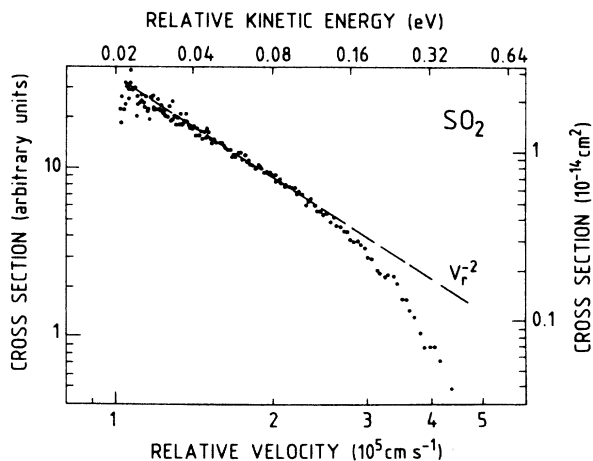


FIG. 6. Experimental ionization cross section $\sigma_i^{\text{exp}}(v_r)$ for $\text{He}(14^1P) + \text{SO}_2$ collisions (as in Fig. 5).

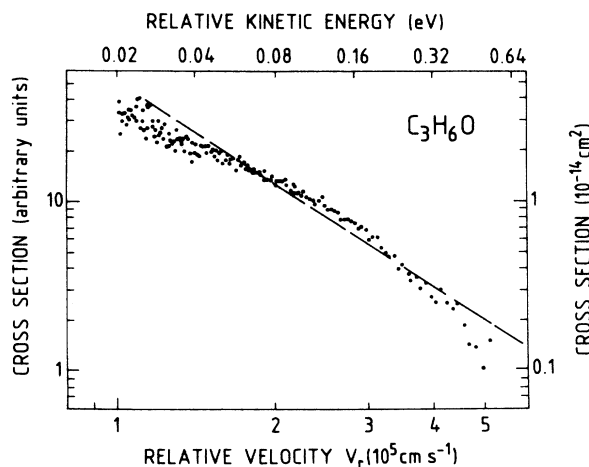
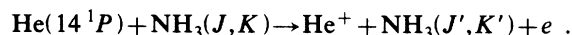


FIG. 7. Experimental ionization cross section $\sigma_i^{\text{exp}}(v_r)$ for $\text{He}(14^1P) + \text{C}_3\text{H}_6\text{O}$ collisions (as in Fig. 5).

A. Origin of the He^* ionization energy

The first comment concerns the origin of the energy which is transferred to the Rydberg atom to ionize it. Let us consider the energy balance of the reaction



The conservation of total energy leads to

$$E^* + E_{J,K} + E_{\text{kin}}^i = E^+ + E_{J',K'} + \varepsilon + E_{\text{kin}}^f , \quad (10)$$

where $E^+ - E^* = |E_{nl}|$ is the ionization energy of the Rydberg atom [for $\text{He}(14^1P)$, $|E_{nl}| = 558.8 \text{ cm}^{-1}$], E_{kin}^i and E_{kin}^f are the kinetic energies of relative motion of the Rydberg-atom-molecule system in the incoming channel and of the ion-molecule system in the outgoing channel, respectively. The electron removes the energy ε as kinetic energy; its minimum is $\varepsilon = 0$ where the electron is ejected without kinetic energy. In this case

$$\Delta E_{\text{rot}} + \Delta E_{\text{kin}} \geq |E_{nl}| . \quad (11)$$

Here, $\Delta E_{\text{rot}} = E_{J,K} - E_{J',K'}$ is the quantity of rotational energy available from deexcitation of the molecule, and $\Delta E_{\text{kin}} = E_{\text{kin}}^i - E_{\text{kin}}^f$ is the quantity of kinetic energy released in the collision which could be used for ionization of He^* . If the ionization process had its origin in a kinetic energy transfer, a threshold should be observed in the cross-section behavior versus v_r as soon as the relative kinetic energy of the reactants available in the incoming channel is sufficient. This threshold would take place around $E_{\text{kin}}^i \approx 558.8 \text{ cm}^{-1}$, then $v_r \approx 2060 \text{ m/s}$. We observe no such phenomenon.

Furthermore, we have performed the same experiment on CO and NO, the dipole moments of which are very small (for CO, $D = 0.10 \text{ D}$; for NO, $D = 0.07 - 0.16 \text{ D}$), and on nonpolar molecules such as O_2 and (1-3) butadiene (C_4H_6); no signal could be measured. This signifies that the prevailing interaction is that with the dipole; this had been mentioned in several experiments on high-Rydberg-state-atom-atomic or molecular target collisions. With

atomic targets and nonpolar molecules, only l mixing corresponding to extremely small energy transfers (less than 1 cm^{-1}) is observed, while n changing appears as soon as the molecule possesses even a small dipole moment¹⁸ which introduces a very efficient long-range interaction term in the potential. Therefore we can conclude that the ionization observed in the present experiment is certainly not due to a transfer of kinetic energy from the relative motion of the colliding system to the Rydberg electron.

B. Comments on the use of the free-electron model

The velocity dependence is not a $1/v_r$ dependence as would be expected after considering the free-electron model. Such $1/v_r$ dependence appears very clearly in the relevant analytical formulas given by Petitjean and Gounand,⁵

$$\sigma_{\text{ion}}^d(nl, J \rightarrow J-1) = \frac{2^{11} n D^2}{135 v_r} \frac{J}{2J+1} \left(1 - \frac{3}{7}\beta + \frac{2}{7}\beta^2\right). \quad (12)$$

Here $\beta = 2n^2 \varepsilon_0$ and ε_0 is the maximum energy released to the ejected electron $\varepsilon_0 = \Delta E_{\text{rot}} - |E_{nl}|$ [formula (12) is valid for $\beta < 0.4$; if $\beta > 0.4$ the last term in parentheses of formula (12) is a more complicated expression but the $1/v_r$ dependence of σ_{ion}^d still exists]. In this model (see Ref. 19, and references therein), the three-body (electron e , core A^+ , molecule M) transition operator $T = T_{e-M} + T_{A^+-M} + C_{\text{imp}} + C_{\text{MS}}$ is reduced to the first term T_{e-M} . The first simplification step concerns the last two terms, C_{imp} (impulse corrective term) and C_{MS} (multiple-scattering term): these terms are disregarded in the frame of the impulse approximation (IA), then $T = T_{e-M} + T_{A^+-M}$. The second simplification step consists in disregarding the core-molecule interaction term T_{A^+-M} , leading to the simple expression $T = T_{e-M}$ which is the starting point of the free-electron model.

However, such simplifications imply the fulfillment of certain conditions, in particular, the IA is justified if the interaction times t_{e-M} and t_{A^+-M} are very small compared to the $e-A^+$ interaction characteristic time t_{e-A^+} (which is the period of the Rydberg electron on its orbit t_n), i.e.,

$$t_{e-M} \ll t_n, \quad (13a)$$

$$t_{A^+-M} \ll t_n. \quad (13b)$$

We can express (i) the electron-molecule interaction time by $t_{e-M} = r_{e-M}/v_n$, since the electron-molecule relative velocity is taken as being equal to that of the electron on its orbit,²⁰ v_n , for our thermal velocity range (1100–5500 m/s, which corresponds to 5 to 25×10^{-4} a.u.), and (ii) the core-molecule interaction time by $t_{A^+-M} = r_{A^+-M}/v_r$, since the core-molecule relative velocity is equal to the He^* -molecule relative velocity defined in the present paper by v_r (all these characteristic values are mean values). Therefore the inequality (13) gives, in the frame of the interaction distances,

$$r_{e-M} \ll t_n v_n, \quad (14a)$$

$$r_{A^+-M} \ll t_n v_r. \quad (14b)$$

Orders of magnitude of (14) can be deduced from the scaling laws relative to Rydberg states: $t_n = 2\pi n^3$ a.u. (for circular orbits, which is not exactly the case here) and $v_n = 1/n$ a.u. In the case $n=14$, $t_n \approx 1.7 \times 10^{+4}$ a.u. ($\approx 4.2 \times 10^{-13}$ s) and $t_n v_n = 2\pi n^2$ a.u. is of the order of $1200a_0$; therefore, it is highly probable that requirements for inequality (14a) relevant to electron-molecule interaction will be satisfied. This is not so for (14b) because of the low collision velocity: $t_n v_r \approx 9a_0$ at the lower limit of our velocity range and the requirements for inequality (14b) are unlikely to be satisfied. Use of the IA is consequently questionable for such systems at thermal velocities. For a more precise discussion, the absolute values of the cross sections, giving an estimation of the interaction ranges, would have to be known. This is one of the reasons which encouraged us to measure them in spite of the difficulties of reaching absolute values in a crossed-beam apparatus using counting techniques. These absolute values are presented in the following paper.²¹

As suggested by Preston and Lane²² in their recent classical study of the Rydberg-atom–HF or Rydberg-atom–HCl system, multiple electron-molecule encounters may occur as a direct consequence of the small value of $t_n v_r$, as given above: during one orbital period of the Rydberg electron, the molecule has time to move a distance of $\Delta l \approx t_n v_r$, and if this distance is smaller than the size of the interaction region, the electron and molecule can interact a second time or more. Preston and Lane note that even at n as high as 40, due to the large interaction size, such multiple encounters may occur. Apart from consideration of a possible core-molecule interaction, such multiple electron-molecule encounters could be introduced in the free-electron model. It would be interesting to look at the behavior of the resulting cross section as a function of the relative velocity v_r .

C. Conclusion

It is clear, from the discussion above, that the collisional ionization in such low(n)-Rydberg-state-atom–molecule collisions cannot be simply interpreted on the basis of the free-electron model in its simpler version including the dipole-Born approximation. This system, where n is as low as 14, certainly represents a severe test of the limits of the free-electron model. On the one hand, the dipole-Born approximation, resulting in $|\Delta J| = 1$ $\Delta K = 0$ rotational transitions, used in this model to treat the electron-molecule interaction, is unable to explain the ionization of such low levels. As noted in our previous paper,¹⁰ we observed better interpretation of rotational excitation of molecules by free electrons using the dipole-Glauber approximation,²³ allowing the $|\Delta J| > 1$ forbidden transitions in the dipole-Born approximation. In this direction, Shirai and Nakamura²⁴ have calculated dipole-Glauber ionization cross sections within the frame of the free-electron model for the systems $\text{Xe}^* + \text{CO}$, HCl , HF , and LiF . They show that, for low excited Rydberg atoms ($n \approx 20$), contributions to ionization with

$|\Delta J| > 1$ transitions prevail over those with dipole-allowed $|\Delta J| = 1$, $\Delta K = 0$ transitions. However, the cross section calculated in the Glauber approximation varies in v_r^{-1} , like that calculated in the dipole-Born approximation, and does not match our data. Perhaps, consideration of multiple electron-molecule encounters during one collision could better explain the experimental data. If not, the core-molecule interaction so far disregarded should be taken into account. This experiment consequently shows explicitly that the free-electron model in its usual version would only appear to be suitable for the interpretation of quite-high(n) (in thermal collisions, $u > 40$ at least)-Rydberg-state atom-molecule collisions. However, the unavailability of a more refined but easy-to-use model is certainly the reason for using this model for Rydberg atoms as low as $n = 20$.

According to the discussion in Sec. IV B, the absolute values of the collisional-ionization cross sections would appear to be an important parameter for checking of the inequalities (14), enabling conclusions to be reached as to the applicability of the impulse approximation in the present case. Such a measurement and the consequent discussion are described in the following paper.²¹

ACKNOWLEDGMENTS

We gratefully thank Dr. F. Gounand, Professor H. Nakamura, and Professor M. Matsuzawa for fruitful discussions and comments on this experiment and results. It is a pleasure to acknowledge D. Sevin for her help on the microcomputer programs and F. Thoyer for improving the lambda-meter performances.

¹See, for instance, *Rydberg States of Atoms and Molecules*, edited by R. F. Stebbing and F. B. Dunning (Cambridge University Press, Cambridge, England, 1983).

²M. Matsuzawa, *J. Chem. Phys.* **55**, 2685 (1971); **58**, 2674 (1973); *J. Phys. Soc. Jpn.* **32**, 1088 (1972); **33**, 1108 (1972); *J. Electron Spectrosc. Relat. Phenom.* **4**, 1 (1974); *J. Phys. B* **8**, 2114 (1975); *Phys. Rev. A* **18**, 1396 (1978); **20**, 860 (1979); *J. Phys. B* **17**, 795 (1984); see also, for a discussion of this model, for example, articles by M. Matsuzawa and by A. P. Hickman, R. E. Olson and J. Pascale, in *Rydberg States of Atoms and Molecules*, edited by R. F. Stebbings and F. B. Dunning (Cambridge University Press, Cambridge, England, 1983).

³M. R. Flannery, *Ann. Phys. (N.Y.)* **61**, 465 (1970); **79**, 480 (1973).

⁴C. J. Latimer, *J. Phys. B* **10**, 1889 (1977).

⁵F. Gounand and L. Petitjean, *Phys. Rev. A* **30**, 61 (1984); L. Petitjean and F. Gounand, *ibid.* **30**, 2946 (1984).

⁶F. G. Kellert, K. A. Smith, R. D. Rundel, F. B. Dunning, and R. F. Stebbings, *J. Chem. Phys.* **72**, 3179 (1980).

⁷C. Higgs, K. A. Smith, G. B. McMillian, F. B. Dunning, and R. F. Stebbings, *J. Phys. B* **14**, L285 (1981).

⁸A. Kalamarides, L. N. Goeller, K. A. Smith, F. B. Dunning, M. Kimura, and N. F. Lane, *Phys. Rev. A* **36**, 3108 (1987).

⁹L. Petitjean, F. Gounand, and P. R. Fournier, *Phys. Rev. A* **33**, 143 (1986); **33**, 1372 (1986).

¹⁰A. Pesnelle, C. Ronge, M. Perdrix, and G. Watel, *Phys. Rev. A* **34**, 5146 (1986).

¹¹See, for example, A. Pesnelle, G. Watel, and C. Manus, *J. Chem. Phys.* **62**, 3590 (1975); J. Fort, J. J. Laucagne, A. Pesnelle, and G. Watel, *Chem. Phys. Lett.* **37**, 60 (1976); *Phys. Rev. A* **14**, 658 (1976); **18**, 2063 (1978).

¹²A. Pesnelle and S. Runge, in *Invited Papers of the Thirteenth International Conference on the Electronic and Atomic Physics*

of Collisions, Berlin, 1983, edited by J. Eichler, I. V. Hertel, and N. Stolterfoht (North-Holland, Amsterdam, 1984), p. 559.

¹³A. Pesnelle, S. Runge, M. Perdrix, D. Sevin, and G. Watel, *J. Phys. B* **16**, L193 (1983); S. Runge, A. Pesnelle, M. Perdrix, G. Watel, and J. S. Cohen, *Phys. Rev. A* **32**, 1412 (1985).

¹⁴S. Runge, A. Pesnelle, M. Perdrix, D. Sevin, N. Wolffer, and G. Watel, *Opt. Commun.* **42**, 45 (1982).

¹⁵C. E. Theodosiou, *Phys. Rev. A* **30**, 2910 (1984).

¹⁶C. E. Theodosiou, *At. Data Nucl. Data Tables* **36**, 97 (1987).

¹⁷*Molecular Spectra and Molecular Structure II. Infrared and Raman Spectra of Polyatomic Molecules*, edited by G. Herzberg (Van Nostrand, New York, 1966).

¹⁸L. Petitjean, F. Gounand, and P. R. Fournier, *Phys. Rev.* **30**, 736 (1984).

¹⁹F. Gounand and L. Petitjean, *Phys. Rev. A* **32**, 793 (1985).

²⁰The electron-molecule relative velocity is given by $v_{e-M} = v_{e-A} + m_A / (m_A + m_e) - v_r$, where v_{e-A} is the velocity of the electron in its orbit, named v_n in the approximation of the circular orbits, and equal to $2.2 \times 10^8 / n$ cm/s: for $n = 14$, $v_n = 1.6 \times 10^7$ cm/s. For our thermal collisions ($10^5 < v_r < 5 \times 10^5$ cm/s) v_r is negligible compared to v_n . Since $m_e \ll m_A$, one has $v_{e-M} = v_n$.

²¹A. Pesnelle, C. Ronge, M. Perdrix, and G. Watel, following paper, *Phys. Rev. A* **38**, 4560 (1988).

²²S. Preston and N. F. Lane, *Phys. Rev. A* **33**, 148 (1986).

²³N. F. Lane, *Rev. Mod. Phys.* **52**, 4544 (1980), Secs. III C and III E; I. Shimamura, in *Electron-Molecule Collisions*, edited by I. Shimamura and K. Takayanagi (Plenum, New York, 1984), pp. 89-189; K. Onda, *J. Phys. Soc. Jpn.* **54**, 4544 (1985).

²⁴T. Shirai and H. Nakamura, *Phys. Rev. A* **36**, 4290 (1987).